Materials Physics and Mechanics 44 (2020) 316-323 Received: July 29, 2020

CONTROL OF (AL,GA)P COMPOSITION IN SELF-CATALYZED NANOWIRE GROWTH

Nickolay V. Sibirev[1], Vladimir Fedorov[2], Igor V. Shtrom[3], Alexey D. Bolshakov[1,4], Yury Berdnikov[1*]

[1]ITMO University, 49 Kronverksky pr., St. Petersburg 197101, Russia

[2]Peter The Great St. Petersburg Polytechnic University, Polytechnicheskaya 29, St. Petersburg 195251, Russia

[3]St. Petersburg State University, Universitetskaya emb. 7/9,199034 St. Petersburg, Russia

[4]Alferov University, Khlopina 8/3, St. Petersburg 194021, Russia

*e-mail: yury.berdnikov@itmo.ru

Abstract. Composition of ternary III-V nanowires became a subject of recent intensive studies inspired by several optoelectronic applications. Among these nanostructures, phosphide nanowires possess a wider bandgap making it especially promising for applications operating in the green visible range. However, unlike other III-V materials, the growth of AlGaP nanowires remains rather unexplored. In this work, we model the stationary composition of self-catalyzed AlGaP grown by molecular beam epitaxy. We show that under a wide range of growth parameters our theoretical approach does not require any fitting parameter and thus allows direct interpretation of experimental data. The obtained numerical results demonstrate a tendency to Al domination over Ga at rather low fluxes of the first. Interesting phenomena of the rise of Al fraction with an increase of the total group III flux is demonstrated. On the other hand, high tolerance of the chemical composition to the temperature, concentration of phosphorus in the droplet, and adatom kinetics is shown numerically.

Keywords: gallium arsenide phosphide, ternary nanowire, composition modeling

1. Introduction

Opportunities for combining different materials in III-V nanowires (NWs) nowadays enable various photonic and optoelectronic applications in devices with novel functionality [1-3]. In the case of ternary III-V compounds, most device applications require compositional control during the synthesis to obtain ensembles of heterostructured NWs with unique electronic and optical properties such as large-area p-n junctions in core-shell geometry and Bragg reflectors for the fabrication of nanosized sources of laser radiation.

Molecular beam epitaxy (MBE) is one of the widely used highly controllable approaches to III-V NW synthesis via so-called vapor-liquid-solid (VLS) growth which implies the metallic nanodroplets to act as the growth catalysts. The catalyst droplets may be composed of either foreign metal (usually Au) or group three material [4]. The latter case, which is called the self-catalyzed growth, may be preferred for applications since it prevents any unintentional contamination of III-V structure with the foreign catalyst species.

Despite the advantage of the higher purity of the self-catalyzed NWs, the problem of the control over the crystalline phase and the well-known effect of the polytypism becomes more prominent due to the inability to govern the shape of the droplet and concentration of each

http://dx.doi.org/10.18720/MPM.4432020_4

growth specie separately. As the chemical composition of the NW can affect its phase purity, the development of the theoretical models of the alloyed NW growth becomes especially important.

Among other III-Vs, phosphide NWs are known for larger bandgaps and low optical losses. Although GaP is one of the well-established semiconductor materials, its ternary alloys are not systematically studied. AlGaP typically possesses a zincblende crystal structure with an indirect bandgap in thin films or in bulk. In contrast, AlGaP NWs can be synthesized in the wurtzite crystal phase with a direct bandgap allowing for the development of light-emitting devices operating in the green color region [5,6].

Despite active studies of ternary III-V NWs [7-9], up to now, there have been reported no growth modeling which allows calculation of AlGaP NW composition. In this work, we study theoretically the self-catalyzed growth of ternary AlGaP NWs to explore the effect of the growth parameters and develop the model for precise compositional control of AlGaP NW by tuning the atomic flux ratio.

2. Model

We consider the VLS MBE growth of ternary $Al_xGa_{1-x}P$ NWs from the droplets of the ternary liquid alloy (Al-Ga-P). Figure 1 illustrates the complex transport of the growth species. We account for direct impingement to the droplet of Al and Ga atoms and P_2 molecules (1), diffusion fluxes of Al, Ga from and to NW sidewalls (2 and 3), incorporation of Ga-P and Al-P pairs into the NW (4), and P evaporation from the droplet.

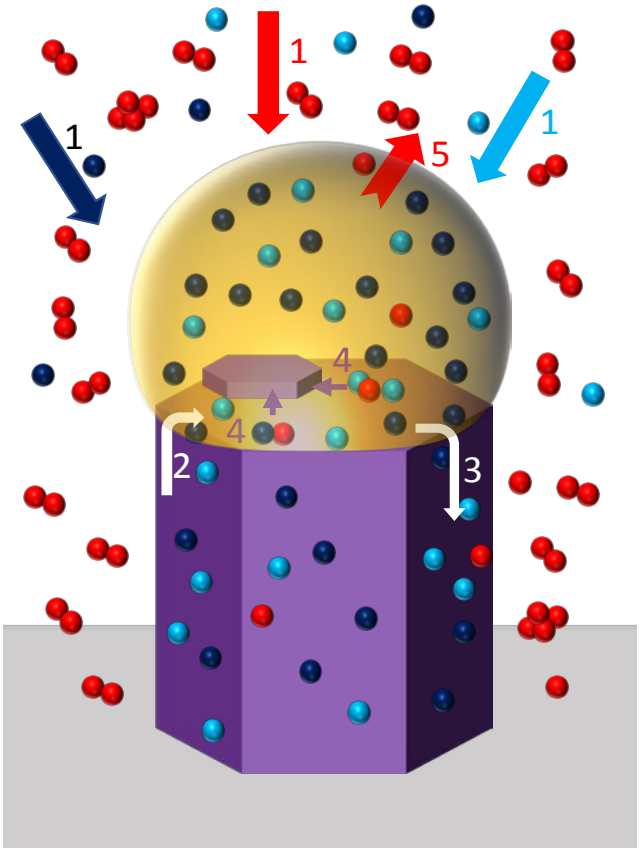

Fig. 1. Schematics of NW growth via VLS mechanism: (1) direct impingement of Ga, Al, and P from material flux, (2) diffusion of Ga and Al adatoms from NW sidewalls to the catalyst, (3) reverse Ga and Al adatom flux from droplet to the NW sidewalls, (4) incorporation of Ga-P and Al-P pairs into the step of an incomplete monolayer, (5) evaporation of P atoms from the droplet

To obtain analytically the growing NW composition *x*, we assume the layer-by-layer growth regime which is typical for the epitaxial formation of the NWs. In this case, the composition of a new monolayer (ML) of $Al_xGa_{1-x}P$ is given by the ratio of incorporation rates corresponding to AlP (v_{AlP}) and the sum of GaP (v_{GaP}) and AlP (v_{AlP}), according to [10,11]:

$$x = \frac{v_{AlP}}{v_{AlP}+v_{GaP}}. \quad (1)$$

As previously shown in [10], the incorporation rates can be found as functions of chemical activities, which, in turn, are defined by the difference in chemical potential of solid and liquid phases $\Delta\mu_{AlP}$ and $\Delta\mu_{GaP}$ as[12]:

$$v_{AlP} = G_{AlP}(exp(\Delta\mu_{AlP}) - 1), \quad (2a)$$

$$v_{GaP} = G_{GaP}(exp(\Delta\mu_{GaP}) - 1), \quad (2b)$$

where G_{AlP} and G_{GaP} are exponential prefactors for AlP and GaP respectively. The latter ones are primarily determined by the growth kinetics and thus are considered equal. Chemical potential differences $\Delta\mu_{AlP}$ and $\Delta\mu_{GaP}$ can be expressed as composition-dependent potential in the droplet μ_α ($\alpha = Ga, Al$ or P) and independent $\Delta\mu^0_{AlP}$ $\Delta\mu^0_{GaP}$ terms [12,13]:

$$\Delta\mu_{AlP} = -\Delta\mu^0_{AlP} + \mu_{Al} + \mu_P, \quad (3a)$$

$$\Delta\mu_{GaP} = -\Delta\mu^0_{GaP} + \mu_{Ga} + \mu_P. \quad (3b)$$

The composition-independent terms could be found as functions of growth temperature T expressed in K [14]: $\Delta\mu^0_{GaP} = -2.983\ln(T) - 8.56 * 10^{-5}T + 17.133 - 7913T^{-1} + 17622T^{-2} + \ln(1-x)$ and $\Delta\mu^0_{AlP} = 2.774\ln(T) - 1.724 * 10^{-4}T - 28.884 - 8212T^{-1} + 121713T^{-2} + \ln(x)$. The binary coefficient for GaP and AlP in the solid phase is negligible [15]. The composition-dependent terms can be found as the functions of elemental concentrations inside the droplet C_α ($\alpha = Ga, Al$ or P) [15]:

$$\mu_\alpha = ln(C_\alpha) + \omega_{\alpha\beta}{C_\beta}^2 + \omega_{\alpha\gamma}{C_\gamma}^2 + C_\beta C_\gamma(\omega_{\alpha\beta} + \omega_{\alpha\gamma} - \omega_{\beta\gamma}), \quad (4)$$

with the temperature-dependent binary coefficients $\omega_{AlP} = -1.01 + 884/T$, $\omega_{GaP} = -2.192 + 1622/T$, $\omega_{GaAl} = 52.53/T$ [15], where T is the substrate temperature during the growth, expressed in K. The concentrations of alternating group III elements Al and Ga (C_{Al} and C_{Ga}) may be calculated with the use of material balance equations in stationary P-limited growth regime [16,17]:

$$F_{Al} + 2\frac{\lambda_{Al}}{R}\chi_1 F_{Al} - 2\frac{D_{Al}}{R\lambda_{Al}}\chi_2 C_{Al} = xF_P, \quad (5a)$$

$$F_{Ga} + 2\frac{\lambda_{Ga}}{R}\chi_1 F_{Ga} - 2\frac{D_{Ga}}{R\lambda_{Ga}}\chi_2 C_{Ga} = (1-x)F_P. \quad (5b)$$

Here F_{Al} and F_{Ga} are the direct impingement flux rates of Al and Ga, respectively, expressed in ML/s, F_p is the resultant phosphorus influx rate, R is the NW radius, D_α and λ_α are the adatom diffusion coefficients and diffusion lengths on NW sidewalls, χ_1 and χ_2 are geometry-dependent coefficients. The first term in the left-hand side of each equation corresponds to the direct impingement. The second term describes the diffusion from the sidewalls to the droplet. The third term describes the reverse concentration-dependent diffusion flux from the droplet. The right-hand side stands for the crystallization rate of binary compounds. We note that evaporation could be neglected [18] in accounting the group III adatom transport on the sidewalls at typical temperatures of (Al,Ga)P NWs growth (400 – 600°C) [6,19,20]. Therefore λ_{Ga} and λ_{Al} are both limited by the adatom incorporation into the NW sidewalls governed by the step-flow radial growth and thus both have similar values [21,22].

Equations (5a) and (5b) can be combined to express the C_{Ga}/C_{Al} ratio as the function of effective flux ratios $f_{Al/Ga} = F_{Al}/F_{Ga}$ and $f_{III/V} = [F_{Ga}(1 + 2\chi_1\lambda_{Ga}/R) + F_{Al}(1 + 2\chi_1\lambda_{Al}/R)]/F_P$ as

$$\frac{C_{Ga}}{C_{Al}} = \frac{D_{Al}}{D_{Ga}}\frac{\lambda_{Ga}}{\lambda_{Al}}\frac{f_{III/V}-(1-x)(1+f_{Al/Ga})}{f_{Al/Ga}f_{III/V}-x(1+f_{Al/Ga})}. \quad (6)$$

Here the coefficient $(1+2\chi_1\lambda_\alpha/R)$ characterizes the effective flux of group III adatoms to the NW top, which includes both direct impingements to the droplet and the sidewall diffusion.

3. Results and discussion

The system of Equations (1) – (6) can be used to calculate the NW composition x as the function of flux ratios $f_{Al/Ga}$ and $f_{III/V}$ with the two parameters: C_p and $\tau = \frac{D_{Al}}{D_{Ga}}\frac{\lambda_{Ga}}{\lambda_{Al}}$. However, as we show further, in the case of AlGaP material system, the composition should be independent of both parameters, and thus, the system of Eqns. (1) - (6) can be solved self-consistently without any fitting. In our calculations, we first assume $\tau = 1$ which is equivalent to the growth conditions at which the values of D_{Al} and D_{Ga} are close [21,23]. And further, we discuss the role of τ separately.

Solving the system of equations numerically we obtain the dependence of the composition x on the flux ratio $f_{Al/Ga}$ (Fig. 2) for a given temperature and C_P. Figure 2 shows that if $f_{III/V} = 4$ and the growth temperature $T = 450$°C Al concentration increases up to almost 1 at $f_{Al/Ga}$ below 0.4. Low Ga incorporation can be explained by higher Gibbs free energy of formation of the compound for AlP ($\Delta\mu^0_{AlP} \approx -22$) in comparison with the value for GaP ($\Delta\mu^0_{GaP} \approx -13$) [14]. Thus, the difference in chemical potentials of solid and liquid phases for Ga-P pair is much smaller than for Al-P pair for similar Ga and Al concentrations. Therefore, the incorporation rate according to Eq. (2) for Al atoms would be greater than for Ga atoms.

Interestingly, the saturation value of $f_{Al/Ga}$ corresponding to pure AlP shifts right at lower $f_{III/V}$ and left at higher $f_{III/V}$ as illustrated in Fig. 2.

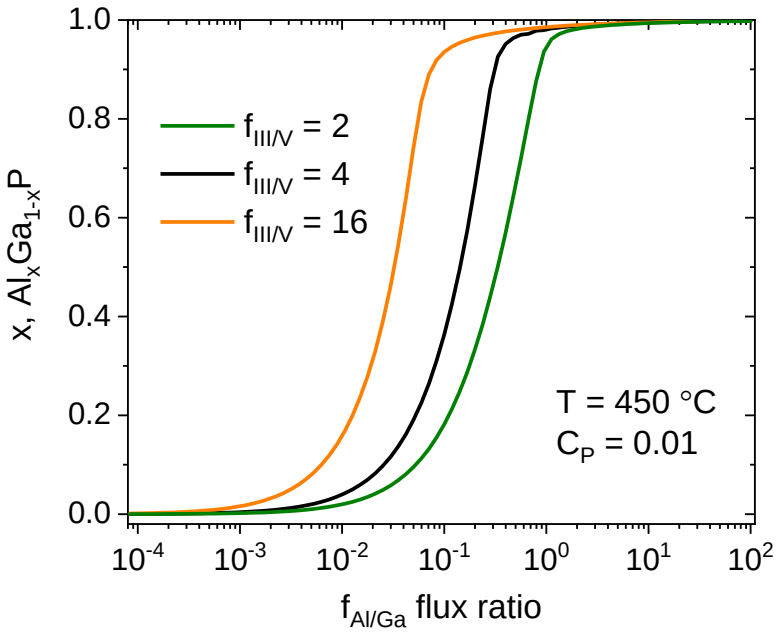

Fig. 2. Calculated composition of $Al_xGa_{1-x}P$ NWs as the function of the Al/Ga flux ratio at different $f_{III/V}$, the growth temperature of 450ºC and $C_P = 0.01$

Next, we study the influence of the phosphorus concentration in the droplet. The latter value can be considered as an unknown parameter and typically is the subject of speculation.

As illustrated in Fig. 3 the results of calculations are found to be independent of the exact value of phosphorus concentration thus making the results of the modeling trustworthy.

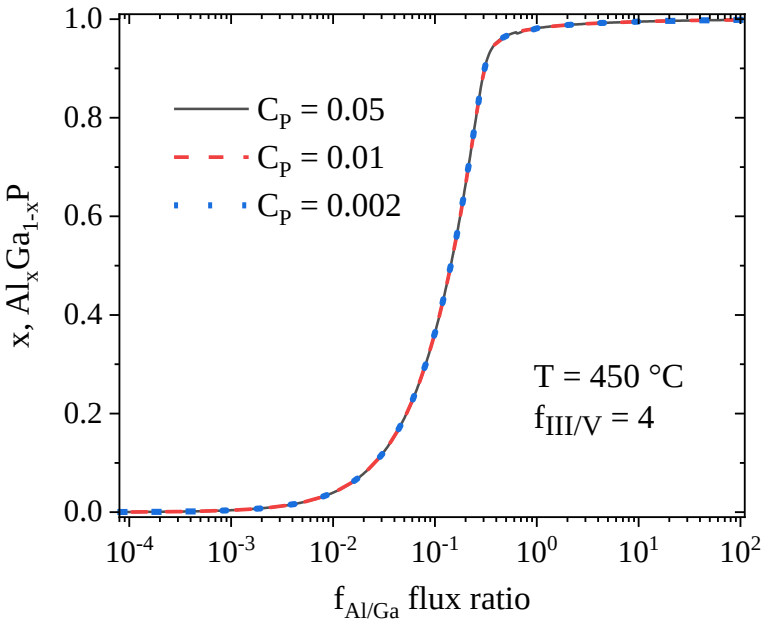

Fig. 3. Calculated chemical composition of $Al_xGa_{1-x}P$ NWs as the function of the Al/Ga flux ratio at different phosphorus concentrations in the liquid phase, the growth temperature of 450ºC and $f_{III/V} = 4$

From a mathematical point of view, we can explain the obtained results by considering Eqns. (3), which could be expressed in the form $\Delta\mu_{\alpha\beta} = -\Delta\mu^0_{\alpha\beta} + ln(C_\alpha) + ln(C_\beta) + P(C_\alpha, C_\beta, C_\gamma)$, where $P(C_\alpha, C_\beta, C_\gamma)$ is a homogeneous quadratic polynomial. We note that $P(C_\alpha, C_\beta, C_\gamma)$ is considerably smaller than the concentration-independent term $-\Delta\mu^0_{\alpha\beta}$. Neglecting the $P(C_\alpha, C_\beta, C_\gamma)$ brings proportionality of both incorporation rates v_{GaP} and v_{AlP} to C_P according to Eq. (2). The insertion of the incorporation rates into denominator and numerator of the right-hand side of Eq. (1) leads to almost no dependence of the NW composition x on C_P.

From a physical point of view, small $P(C_\alpha, C_\beta, C_\gamma)$ values correspond to weak interactions inside the ternary alloy and therefore weak impact of phosphorus on the composition of $Al_xGa_{1-x}P$ NWs. We should also note that the considered type of chemical potentials can be found in other fields of condensed matter physics such as thin film growth [24,25] or processes of spinodal decomposition [26,27].

Figure 4 shows that this effect has almost no temperature dependence due to weak logarithmic dependence of the chemical potential difference on temperature.

So far, we assumed $\tau = 1$. In the more general case, the value of τ is affected by diffusion coefficients for group III adatoms on the NW sidewalls, which depend on many parameters such as the growth temperature, facet orientation, roughness, and so on. However, as we show in Fig. 5, even ten times the variation in τ leads only to a slight change in x below a few percent.

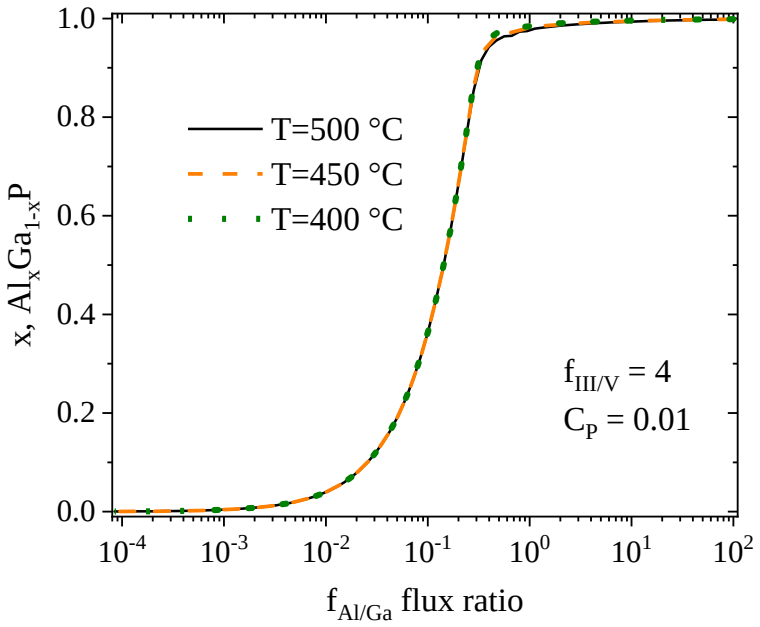

Fig. 4. Calculated composition of $Al_xGa_{1-x}P$ NWs as the function of the Al/Ga flux ratio at different growth temperatures, $f_{III/V} = 4$ and $C_P = 0.01$

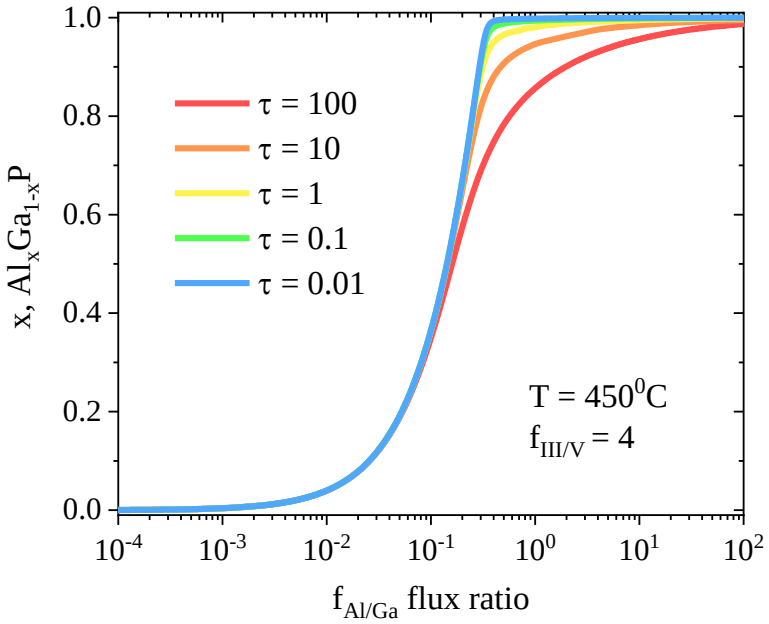

Fig. 5. Calculated composition of $Al_xGa_{1-x}P$ NWs as the function of the Al/Ga flux ratio at different τ, the growth temperature of 450ºC, $f_{III/V} = 4$ and $C_P = 0.01$

6. Conclusions

Summing up, we conclude that within our approach we obtain the self-consistent model of the self-catalyzed AlGaP NWs stationary formation in MBE process. Our modeling explains the ways to control the NW composition by variation of the growth fluxes. The model results demonstrate the anticipated tendency to preferential incorporation of Al to Ga. Interestingly, the model predicts an increase of the Al molar fraction with the total group III flux at a fixed Al/Ga flux ratio. We show that the chemical composition of the NWs does not depend on phosphorus concentration, the kinetics of the growth species on the NW sidewalls, and temperature within the wide parameter ranges making the control over the composition

technologically feasible. Our model does not require any fitting parameter and thus allows direct interpretation of experimental data.

Acknowledgments*. Authors thank the support from the Russian Ministry of Science and Higher Education under the grant 05.617.21.0058 (project ID RFMEFI61719X0058).*

References

[1] Barrigón E, Heurlin M, Bi Z, Monemar B, Samuelson L. Synthesis and Applications of III–V Nanowires. *Chem Rev.* 2019;119(15): 9170-9220.
[2] Quan LN, Kang J, Ning CZ, Yang P. Nanowires for Photonics. *Chem Rev.* 2019;119(15): 9153-9169.
[3] Mozharov AM, Kudryashov DA, Bolshakov AD, Cirlin GE, Gudovskikh AS, Mukhin IS. Numerical simulation of the properties of solar cells based on GaPNAs/Si heterostructures and GaN nanowires. *Semiconductors.* 2016;50: 1521-1525.
[4] Bolshakov AD, Mozharov AM, Sapunov GA, Fedorov VV, Dvoretckaia LN, Mukhin IS. Theoretical modeling of the self-catalyzed nanowire growth: nucleation- and adsorption-limited regimes. *Mater Res Express.* 2017;4(12): 125027.
[5] Pistol ME, Pryor CE. Band structure of core-shell semiconductor nanowires. *Phys Rev B.* 2008;78(11): 115319.
[6] Assali S, Zardo I, Plissard S, Kriegner D, Verheijen MA, Bauer G, Meijerink A, Belabbes A, Bechstedt F, Haverkort JEM, Bakkers EPAM. Direct band gap wurtzite gallium phosphide nanowires. *Nano Lett.* 2013;13(4): 1559-1563.
[7] Dubrovskii VG. Understanding the vapor–liquid–solid growth and composition of ternary III–V nanowires and nanowire heterostructures. *J Phys D Appl Phys.* 2017;50(45): 453001.
[8] Leshchenko ED, Ghasemi M, Dubrovskii VG, Johansson J. Nucleation-limited composition of ternary III–V nanowires forming from quaternary gold based liquid alloys. *CrystEngComm.* 2018;20: 1649-1655.
[9] Sibirev N V, Timofeeva MA, Bol'shakov AD, Nazarenko MV, Dubrovskii VG. Surface energy and crystal structure of nanowhiskers of III–V semiconductor compounds. *Phys Solid State.* 2010;52: 1531-1538.
[10] Johansson J, Ghasemi M. Kinetically limited composition of ternary III-V nanowires. *RAPID Commun Phys Rev Mater.* 2017;1(4): 40401.
[11] Periwal P, Sibirev NV, Patriarche G, Salem B, Bassani F, Dubrovskii VG, Baron T. Composition-Dependent Interfacial Abruptness in Au-Catalyzed Si 1– x Ge x /Si/Si 1– x Ge x Nanowire Heterostructures. *Nano Lett.* 2014;14(9): 5140-5147.
[12] Bolshakov AD, Fedorov VV, Sibirev NV, Fetisova MV, Moiseev EI, Kryzhanovskaya NV, Koval OY, Ubyivovk EV, Mozharov AM, Cirlin GE, Mukhin IS. Growth and Characterization of GaP/GaPAs Nanowire Heterostructures with Controllable Composition. *Phys Status Solidi – Rapid Res Lett.* 2019;13(11): 1900350.
[13] Dubrovskii VG. Compositional control of gold-catalyzed ternary nanowires and axial nanowire heterostructures based on IIIP1−xAsx. *J Cryst Growth.* 2018;498: 179-185.
[14] Ansara I, Chatillon C, Lukas HL, Nishizawa T, Ohtani H, Ishida K, Hillert M, Sundman B, Argent BB, Watson A, Chart TG, Anderson T. A binary database for III–V compound semiconductor systems. *Calphad.* 1994;18(2): 177-222.
[15] Ilegems M, Panish MB. Phase diagram of the system Al-Ga-P. *J Cryst Growth.* 1973;20: 77-81.
[16] Sibirev NV, Koryakin AA, Dubrovskii VG. On a new method of heterojunction formation in III–V nanowires. *Semiconductors*. 2016;50: 1566-1568.
[17] Dubrovskii VG. A model of axial heterostructure formation in III–V semiconductor nanowires. *Tech Phys Lett.* 2016;42: 332-335.

[18] Detz H, Kriz M, MacFarland D, Lancaster S, Zederbauer T, Capriotti M, Andrews AM, Schrenk W, Strasser G. Nucleation of Ga droplets on Si and SiO x surfaces. *Nanotechnology.* 2015;26(31): 315601.
[19] Berg A, Heurlin M, Tsopanidis S, Stylianos Tsopanidis, Pistol ME, Borgström MT. Growth of wurtzite Al x Ga 1−x P nanowire shells and characterization by Raman spectroscopy. *Nanotechnology.* 2016;28(3): 035706.
[20] Borgström MT, Mergenthaler K, Messing ME, Håkanson U, Wallentin J, Samuelson L, Pistol ME. Fabrication and characterization of AlP-GaP core-shell nanowires. *J Cryst Growth.* 2011;324(1): 290-295.
[21] Sibirev NV, Dubrovskii VG, Arshanskii EB, Cirlin GE, Samsonenko YB, Ustinov VM. On diffusion lengths of Ga adatoms on AlAs(111) and GaAs(111) surfaces. *Tech Phys.* 2009;54: 586-589.
[22] López M, Nomura Y. Surface diffusion length of Ga adatoms in molecular-beam epitaxy on GaAs(100)–(110) facet structures. *J Cryst Growth.* 1995;150: 68-72.
[23] Bonzel HP. *Diffusion in Solid Metals and Alloys*. Berlin: Springer; 1990.
[24] Kukushkin SA, Osipov AV. Thin-film condensation processes. *Physics-Uspekhi.* 1998;41(10): 983-1014.
[25] Dubrovskii VG, Cirlin GE, Bauman DA, Kozachek VV, Mareev VV. Kinetic models of self-organization effects in lattice systems. *Phys A Stat Mech its Appl.* 1998;260(3-4): 349-373.
[26] Skripov VP, Skripov AV. Spinodal decomposition (phase transitions via unstable states). *Sov Phys Uspekhi.* 1979;22(6): 389-410.
[27] Dubrovskii VG. *Nucleation Theory and Growth of Nanostructures.* Berlin: Springer; 2014.